SEARCH FOR QUARKS IN PROTON-PROTON INTERACTIONS AT $\sqrt{s}$ = 52.5 GeV

M. Basile, G. Cara Romeo, L. Cifarelli, A. Contin,
G. D'Ali, P. Giusti, T. Massam, F. Palmonari,
G. Sartorelli, G. Valenti and A. Zichichi

CERN, Geneva, Switzerland
INFN, Sezione di Bologna, Italy
Istituto di Fisica dell'Università, Bologna, Italy

SUMMARY

The results of an experiment to search for quarks in p-p collisions, at a total centre-of-mass energy $\sqrt{s}$ = 52.5 GeV, are reported. The experiment was sensitive to fractionally charged particles with $0.035e \leq |Q| \leq 0.67e$, $\beta = v/c \geq 0.1$, and masses up to 21 GeV/c^2. The 90% confidence level on the ratio "quark flux/charged particle flux" is 5.11×10^{-11} for $|Q|$ = 1/3e. This value holds true for particles produced with a mean transverse momentum of 0.4 GeV/c.

Geneva - 16 January 1978

(Submitted to Nuovo Cimento)

1. INTRODUCTION

We report further results on an experiment performed at the ISR Split-Field Magnet (SFM), to search for fractionally charged particles in high-energy proton-proton collisions. The present work uses data taken at a centre-of-mass energy $\sqrt{s}$ = 52.5 GeV. Previous results referring to higher energy data ($\sqrt{s}$ = 62.2 GeV) have already been published[1].

It should be pointed out that the limit presented here is based on the assumption of proton-breaking mechanisms or quark production processes where a mean transverse momentum p_T of the order of 400 MeV/c is enough. The relevance of this point in the general framework of the quark experiments has been discussed elsewhere[2].

2. EXPERIMENTAL SET-UP AND DATA TAKING

The CERN-Bologna apparatus, shown in Fig. 1 together with the multiwire proportional chambers (MWPC) detector of the SFM, consisted of six plastic scintillation counter hodoscopes positioned symmetrically around the intersection region. The hodoscopes provided an eightfold measurement of dE/dx and time-of-flight of the charged secondaries produced in the p-p collision, while the MWPC system allowed the reconstruction of the tracks in the magnetic field and a measurement of their momentum. Two "Near" hodoscopes (HN and SN) and one "Far" hodoscope (HF) were present in each arm of the apparatus. The Near hodoscopes were made of horizontal "strips" or packs, each of which contained four 2.5 cm thick, 1 m long, scintillation counters. The Far hodoscope strips were vertical. The various widths of the strips, the number of strips in each hodoscope, and the positions of the hodoscopes were determined according to considerations of acceptance and uniformity of rate. The total number of counters used was 208. They were "gradient scintillation counters" [3], particularly suitable for uniform dE/dx measurements along the counter. Each counter was connected to one photomultiplier by a long plexiglas light-guide, which allowed the photomultiplier to be placed in an acceptably low magnetic field region. The light-guides of each strip were covered by a system of "veto" counters to reject events with Čerenkov light production.

As described elsewhere[1], the trigger required the coincidence of at least one "quark candidate" strip signal in a Near hodoscope, at least one "quark candidate" strip signal in the corresponding Far hodoscope of the same arm of the apparatus, and at least one strip signal in any hodoscope of the opposite arm of the apparatus. A strip signal was defined as the coincidence of its four counter signals. A quark candidate strip signal was produced when, in each of the four counters of the strip, the energy loss was between 2% and 60% of the most probable energy loss of a $Q = 1\,e$ minimum ionizing particle (referred to as the "$Q = 1\,e$ peak", in the following). This signal could be vetoed by the signal from the veto counters covering the light-guides of the strip.

The over-all electronic efficiency for fractionally charged particles was evaluated to be 62%.

Data were taken during two separate running periods. The ISR integrated luminosity values together with the corresponding numbers of inelastic beam-beam interactions and of recorded events are given in Table 1. The total integrated luminosity was 2.92×10^{36} cm^{-2}. The trigger rate ranged between 5 and 10 per sec, while the average rate of inelastic beam-beam interactions was of the order of 3×10^5 per sec.

The variation of the trigger rate as a function of the vertical displacement of the beams was very similar to the corresponding variation of the beam-beam rate, as expected from triggers due to beam-beam interactions.

3. ANALYSIS OF THE DATA

3.1 Preselection of the events

The total sample of 3.5×10^6 events was submitted to a preliminary filtering analysis.

i) The trigger conditions were verified in software with a more precise definition of energy loss and timing after time-slewing corrections and pulse-height equalization of the counters had been made.

ii) Accidentals and background contamination were reduced by

a) using as a complementary veto for Čerenkov light signals the information of those regions of the MWPCs which covered the geometrical projection of the light-guides of the strips;

b) rejecting quark candidates involving geometrically incompatible Near-Far pairs of strips;

c) applying a cut to the raw time-of-flight (between Near and Far hodoscopes) of the quark candidate, in order to eliminate random events in which the Far signal was anticipated with respect to relativistic particles;

d) discarding the sample of quark candidates involving the SN hodoscopes in which the background level was found to be an order of magnitude higher than in the HN hodoscopes, despite the fact that the two types of hodoscopes occupied similar angular ranges;

e) identifying a particular kind of background, collectively called "cross-talking" between adjacent strips in the same hodoscope. Such background could come, for example, from sources such as particles which crossed a strip near its boundary, showers or interactions of particles in the hodoscope, producing ionization in two or more adjacent strips, one of which was a low dE/dx candidate.

At this level of the analysis, 5.9×10^3 quark candidates were retained. The efficiency of the preselection was 83%.

3.2 The dE/dx analysis

The eight (four in the Near strip and four in the Far strip) energy loss measurements of the quark candidate were submitted to a "likelihood test", in order to achieve an efficient selection of those events showing a consistent set of dE/dx values. The expected dE/dx probability distribution of particles having charge $|Q| = 1/3e$ and velocity β (= v/c) was calculated by Monte Carlo simulation for each hodoscope counter. The same calculation gave the expected distributions

of the minimum and maximum dE/dx within each strip. These distributions were obtained for seven bins of β which together covered the velocity range accepted by the experiment ($\beta \geq 0.5$ for $|Q| = 1/3e$).

The calculation used the experimental dE/dx probability distribution of normal Q = 1 e particles as input data, and took into account the difference in charge, velocity, and photostatistics.

The expected dE/dx probability distributions $W(PH,\beta)$, where PH = (dE/dx)/(dE/dx of Q = 1 peak), were then used to calculate a likelihood function as follows

$$L(\beta) = \ln\left[W_{min}(PH,\beta)\cdot W_{min}(PH_F,\beta)\cdot W_{max}(PH_N,\beta)\cdot W_{max}(PH_F,\beta)\cdot\prod_{i=1}^{8} W_i(PH_i,\beta)\right]$$

and the distribution of values of $L(\beta)$ was obtained by Monte Carlo integration, for each β-bin. The index i runs over the eight counters in which dE/dx was measured, and $PH_{N(F)}$ stands for the mininum or maximum PH_i present in the Near (Far) strip. When an accidental stop (i.e. an earlier random signal in one of the four counters of a strip, whose three other counters were in time coincidence, causing the loss of information relative to that counter) was found in one of the quark candidate strips, the $L(\beta)$ was expressed in terms of seven PH_i only. Quark candidates having an accidental stop in both Near and Far strips were discarded with 2% efficiency loss. From the $L(\beta)$ distributions obtained for Monte Carlo events, a value $L_{cut}(\beta)$ was chosen such that 90% of the simulated events had $L(\beta) \geq L_{cut}(\beta)$, for each β-bin. The number of bins considered provided uniform acceptance, with an average value of $\sim$ 90%, in the whole velocity range of the experiment (see Fig. 2). The $L(\beta)$ distributions for Monte Carlo and real events are shown in Fig. 3, for all β-bins.

Applying the likelihood test to the quark candidates, allowing them all to be candidates for any β-bin, only 491 survived.

3.3 Analysis of reconstructed events

The events selected by the dE/dx analysis were submitted to the standard SFM reconstruction program chain and examined in detail, introducing the information of the MWPCs as a further tool for background identification.

Several classes of background events were isolated.

i) Events showing, in the chambers in front of or behind the quark candidate strips, an anomalously large number of wire clusters which could not be associated with any visible track pointing to these strips, together with an anomalously large number of counters hit in the same hodoscope as the quark candidate. Such features were interpreted in terms of high background production due to particles interacting in various obstacles such as beam-pipe, frames of the chambers, pillars, magnet pole-faces, upstream compensator magnets, etc. (155 events).

ii) Events showing tracks which had escaped previous detection and crossed the light-guides of quark candidate strips, therefore simulating quark signals by Čerenkov light production (93 events).

iii) Events showing tracks which pointed to the edges of strips which thus appeared as quark candidate strips because of reduced ionization or light collection (99 events).

iv) Events showing very few tracks which did not come from a common vertex inside the intersection volume of the beams. Some even showed only randomly distributed wire clusters which could not represent tracks in the chambers. The time signals were uncorrelated in all hodoscope strips hit. Such events were not due to beam-beam interactions but resulted from interactions of one of the beams with the gas or the wall of the beam-pipe although, as already pointed out, the contamination of such background at the level of the trigger was negligible (17 events).

v) Events in which two consecutive p-p interactions overlapped so that the delayed signals from normal particles produced in the second interaction were only partially recorded on ADC and simulated quark candidate signals (11 events).

We rejected 375 background events in this way. Table 2a gives the number of candidates left in each β-bin subsample. Events accepted in more than one β-bin are counted only once, in the bin corresponding to the highest β value.

3.4 Time-of-flight and velocity analysis

The remaining 116 events, in which no evident source of background could be detected, were finally analysed by means of the time-of-flight (TOF) information. In each event, the true "zero" time of the p-p interaction was derived from the TOF of reconstructed tracks hitting the hodoscopes. On the other hand, since no track associated with the quark candidate strips could be expected (owing to the very low detection efficiency of the MWPC system for $|Q| = 1/3e$ particles), the TOF of the quark candidate could not be corrected for the impact position of the track along the strips and had a large uncertainty. Therefore this TOF could only be analysed in terms of consistency with what was expected for a genuine low-ionizing particle flying from the beams' intersection region to the Near and then to the Far strip. Let us define $TOF_{Int.N}$ as the TOF from the p-p collision vertex to the Near strip, TOF_{NF} as the TOF from the vertex to the Far strip, and $TOF_{Int.F}$ as the TOF from the vertex to the Far strip. The correction for the hit position along the 1 m long strips was $\Delta TOF \leq 7$ nsec. After the application of such correction to $|Q| = 1\,e$ tracks, a time dispersion $\sigma_{TOF}(1\,e) \lesssim 1$ nsec was obtained (see Fig. 4). The expected σ_{TOF} for low-ionizing tracks was evaluated to be $\sigma_{TOF}(1/3e) \simeq 1.5$ nsec. Taking advantage of the fact that each horizontal Near strip projected a band less than 20 cm wide on the vertical Far strips, the $TOF_{Int.F}$ of the quark candidate could be corrected with an uncertainty on ΔTOF of ± 0.8 nsec. The resulting $\sigma_{TOF}(1/3e)$ was ~ 1.7 nsec and the time-base for the Far hodoscopes was ~ 19 nsec, so that the error on the quark candidate velocity determination was $\Delta\beta/\beta \simeq 10\%$ for $\beta = 1$.

The first consistency test applied to the quark candidates was a comparison of $TOF_{Int.N}$ and TOF_{NF}, according to the linear relation existing between them. A scatter plot of the two quantities for all the 116 events is shown in Fig. 5, where the dashed contour defines the fiducial region due to TOF uncertainties.

To the 69 events falling in the "good" region, we applied a second consistency test by checking the compatibility of the velocity (β_{TOF}) derived from the time-of-flight and the velocity attributed to the $|Q| = 1/3e$ candidate by the previous

dE/dx analysis. For each quark candidate, we defined an "overlap function" $u(\beta)$ as follows:

$$u(\beta) = \int_{\beta \geq 0.5} g_{TOF}(\beta)\ h_{PH}(\beta)\ d\beta\ .$$

The function $g_{TOF}(\beta)$ is a normal Gaussian distribution having a mean value equal to β_{TOF} and a standard deviation given by the error on β_{TOF}; $h_{PH}(\beta)$ is the Monte Carlo β probability distribution relative to the β-bin of the event and is the normalized acceptance curve of the bin (see Fig. 2). The $U(\beta) = \ln u(\beta)$ distributions relative to real and Monte Carlo simulated events are shown in Fig. 6, for the various β-bins. By requiring, in each β-bin subsample, $U(\beta) \geq U_{cut}(\beta)$, the value $U_{cut}(\beta)$ being such that more than 90% of the simulated events satisfied this requirement, we selected 14 final candidates. Table 2b gives the β-bin distribution of these events.

In Fig. 7 the 14 events are plotted against their likelihood function value (see Section 3.2). All events belonging to the various β-bin subsamples were grouped in the same graph by shifting the $L(\beta)$ origins so as to make the peaks of the Monte Carlo distribution in Fig. 3 coincide. The full-line curve appearing in Fig. 7 is a best fit of the L probability distribution of the initial 5.9×10^3 background events submitted to the dE/dx analysis, while the dashed-line curve is the corresponding best fit for Monte Carlo events. Both curves were obtained by merging the single β-bin distributions of Fig. 3, using the $L(\beta)$ shifts described above. The probability that the 14 candidates were distributed according to the Monte Carlo was evaluated to be 1.5×10^{-3}. In order to estimate the 90% confidence level upper limit of the number of genuine quark events, we applied a fit to the L distribution of the final candidates. The function used was

$$f_{fit}(L) = n\ f_{MC}(L) + (N-n)\ f_{BG}(L)\ ,$$

where N is the number of quark candidate events; $f_{BG}(L)$ and $f_{MC}(L)$ are the background and the expected Monte Carlo L probability distributions, respectively. We found $n = 0$, $f_{BG}(L)$ producing the total contribution to the fit. The 90% confidence level estimate was: $n_{max}(90\%\ CL) = 6$.

4. RESULTS

4.1 Flux limit

Using the 90% confidence level n_{max} value of Section 3.4, the result of our analysis, expressed in terms of particle ratio limit, is

$$\phi_q/\phi_c < 5.11 \times 10^{-11} \quad (\text{for } |Q| = 1/3e) ,$$

where ϕ_q is the flux of quarks and ϕ_c is the observed flux of charged particles. The error on ϕ_q/ϕ_c was evaluated to be ±10%. This limit is plotted in Fig. 8 together with the limits previously measured at the ISR [1,4] at various centre-of-mass energies.

4.2 Cross-section limit

To obtain a limit on the total cross-section, a model must be assumed. We will keep to the common practice of assuming the production mechanism to be $p + p \to p + p + q + \bar{q}$ with two alternative assumptions. The first assumption, referred to in this paper as the "isotropic" model, is that momenta and angular distributions are given by four-body phase space. The second assumption, referred to as the "p_T limited" model, is that the four-body phase space is weighted by a factor

$$\exp\left(-\sum_{i=1}^{4} p_{T_i}^2/2\langle p_T\rangle^2\right)$$

where $\langle p_T\rangle = 0.4$ GeV/c . Taking into account the fact that only one event out of the 14 examined had a multiplicity of charged tracks consistent with the four-body final state and using the previous assumptions, we computed the 90% confidence level upper limit of the quark production cross-section as a function of the mass. The result is shown in Fig. 9. The most significant limits on $|Q| = 1/3e$ quark production total cross-section[1,4-7] are plotted in Fig. 10 as a function of the centre-of-mass energy. A recent FNAL experiment[8], which does not appear in Fig. 10, was designed to search for quarks produced with a fixed large transverse momentum ($p_T = 2.05$ GeV/c for $|Q| = 1/3e$ at $\sqrt{s} = 27.4$ GeV). As an exercise, we used the same two models to evaluate the result of this experiment in terms of

total cross-section limit. The estimate, for the isotropic model, is of the order of 10^{-36} cm^2, while, for the p_T limited model, it is at least six orders of magnitude higher.

5. CONCLUSION

We have analysed a sample of 3.5×10^6 proton-proton interactions at $\sqrt{s}$ = 52.5 GeV, selected by a trigger sensitive to particles with fractional charge $0.035e \leq |Q| \leq 0.67e$, velocity $\beta = v/c \geq 0.1$, lifetime $\tau > 10^{-8}$ sec, and mass up to 21 GeV/c^2.

The integrated luminosity of our experiment was 2.92×10^{36} cm^{-2}, an order of magnitude higher than in previous ISR experiments, having a comparable solid angle. In addition to ionization and time-of-flight measurements, the experiment took advantage of the multiwire proportional chambers system of the SFM for the event pattern reconstruction.

No evidence for genuine $|Q| = 1/3e$ fractionally charged particles production has been found.

In terms of flux, this experiment sets an upper limit on the "quark flux/charged particle flux" ratio of 5.11×10^{-11} (90% confidence level) which is more than an order of magnitude better than previous results at the same energy. In terms of production cross-section, using for comparison with other experiments the standard production scheme $p + p \rightarrow p + p + q + \bar{q}$ with limited transverse phase-space ($\langle p_T \rangle$ = 0.4 GeV/c), the upper limit of the total production cross-section is $\sigma \lesssim 10^{-35}$ cm^2 (90% confidence level) up to quark masses of 20 GeV/c^2.

REFERENCES

1) M. Basile, G. Cara Romeo, L. Cifarelli, P. Giusti, T. Massam, F. Palmonari, G. Valenti and A. Zichichi, Nuovo Cimento 40A, 41 (1977).

2) M. Basile, G. Cara Romeo, L. Cifarelli, P. Giusti, T. Massam, F. Palmonari, G. Valenti and A. Zichichi, Nuovo Cimento Letters 18, 529 (1977).

3) S.A. Gabriele, P. Giusti, T. Massam, G. Valenti and A. Zichichi, Nuclear Instrum. Methods 108, 431 (1973).

4) C.W. Fabjan, C.R. Gruhn, L.S. Peak, F. Sauli, D.O. Caldwell, L.S. Rochester, U. Stierlin, R. Tirler, B. Winstein and D. Zahniser, Nuclear Phys. 101B, 349 (1975).

5) J.V. Allaby, G. Bianchini, A.N. Diddens, R.W. Dobinson, R.W. Hartung, E. Gygi, A. Klovning, D.H. Miller, E.J. Sacharidis, K. Schlüpmann, F. Schneider, C.A. Stahlbrandt and A.M. Wetherell, Nuovo Cimento 64A, 75 (1969).

6) Yu.M. Antipov, V.N. Bolotov, M.I. Devishev, M.N. Devisheva, V.V. Isakov, I.I. Karpov, Yu.S. Khodyrev, V.A. Krendelev, L.C. Landsberg, V.G. Lapshin, A.A. Lebedev, A.G. Morozov, Yu.D. Prokoshkin, V.A. Rybakov, V.I. Rykalin, A.V. Samojlov, V.A. Senko, N.K. Vishnevsky, F.A. Yetch and A.M. Zajtzev, Phys. Letters 30B, 576 (1969).

7) T. Nash, T. Yamanouchi, D. Nease and J. Sculli, Phys. Rev. Letters 32, 858 (1974).

8) D. Antreasyan, G. Cocconi, J.W. Cronin, H.J. Frisch, L. Kluberg, J. Mueller, K. Olive, P.A. Piroué, M.J. Shochet and R.L. Sumner, Phys. Rev. Letters 39, 513 (1977).

This FNAL experiment is a limited version of a previous proposal of the CERN-Bologna group (ISRC/74-48, 7 October 1974) to search at the ISR for quarks in coincidence with a large-angle electron/hadron calorimeter placed at 90°, i.e. in events with large p_T processes involved.

Table 1

Running period	1	2
Integrated luminosity (cm^{-2})	1.24×10^{36}	1.68×10^{36}
Inelastic beam-beam interactions	4.42×10^{10}	5.98×10^{10}
Collected triggers	1.42×10^{6}	2.07×10^{6}

Table 2

β-bin	(a) Events	(b) Events
$\beta = 0.97$	54	8
$\beta = 0.85$	30	4
$\beta = 0.75$	22	0
$\beta = 0.70$	8	2
$\beta = 0.65$	2	0
$\beta = 0.59$	0	0
$\beta = 0.55$	0	0

Figure captions

Fig. 1 : Top view of the SFM, showing the multiwire proportional chambers and the CERN-Bologna hodoscopes. M = MWPC; S = scintillation counters; P = SFM pole faces; → outgoing beam.

Fig. 2 : β acceptance of the 90% efficient dE/dx selection for each β-bin, corresponding to charge $|Q|$ = 1/3e and velocity value: a) β = 0.97, b) β = 0.85, c) = 0.75, d) β = 0.70, e) β = 0.65, f) β = 0.59, g) β = 0.55.

Fig. 3 : L(β) distributions relative to Monte Carlo and real events, for different β-bins, each corresponding to $|Q|$ = 1/3e and velocity value: a) β = 0.97, b) β = 0.85, c) β = 0.75, d) β = 0.70, e) β = 0.65, f) β = 0.59, g) β = 0.55.

Fig. 4 : Showing the time-of-flight resolution for $|Q|$ = 1e tracks hitting the various hodoscopes: a) HNL (σ_{TOF} = 0.93 nsec), b) HFL (σ_{TOF} = 0.89 nsec), c) HNR (σ_{TOF} = 0.81 nsec), d) HFR (σ_{TOF} = 0.72 nsec).

Fig. 5 : Scatter plot of TOF_{NF} versus $TOF_{Int.N}$ for the events selected in Section 3.3. The compatibility region limited by the dashed line is inclusive of all uncertainties, as discussed in Section 3.4.

Fig. 6 : U(β) distributions relative to real events for different β-bins, each corresponding to charge $|Q|$ = 1/3e and velocity value: a) β = 0.97 (36 events), b) β = 0.85 (19 events), c) β = 0.75 (9 events), d) β = 0.70 (4 events), e) β = 0.65 (1 event). Superimposed are the expected U(β) distributions obtained by Monte Carlo simulation.

Fig. 7 : L distribution of the 14 final events. The full-line and dashed-line curves (each normalized to 14 events) show, respectively, the behaviour of background and Monte Carlo events as a function of L.

Fig. 8 : The flux limits of this experiment compared with existing ISR measurements[1,4] at various energies.

Fig. 9 : The 90% confidence level upper limit of Q = ±1/3e quark production cross-sections as functions of the quark mass, for isotropic and p_T limited ($\langle p_T \rangle$ = 0.4 GeV/c) models.

Fig. 10 : Present status of Q = ±1/3e quark production cross-section as a function of $\sqrt{s}$, from accelerators[5-7] and ISR[1,4] experiments. The "bars" represent the cross-section variation in the quark mass range explored by each experiment.

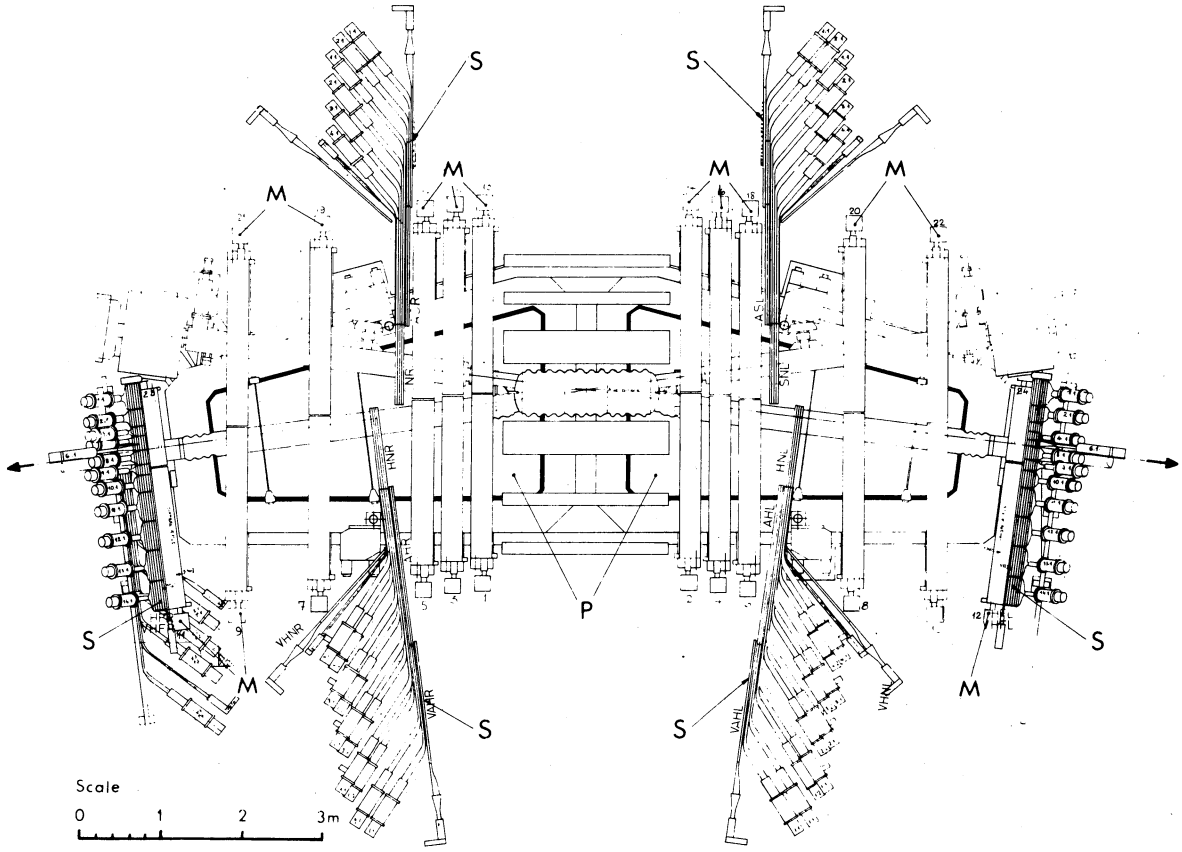

Fig. 1

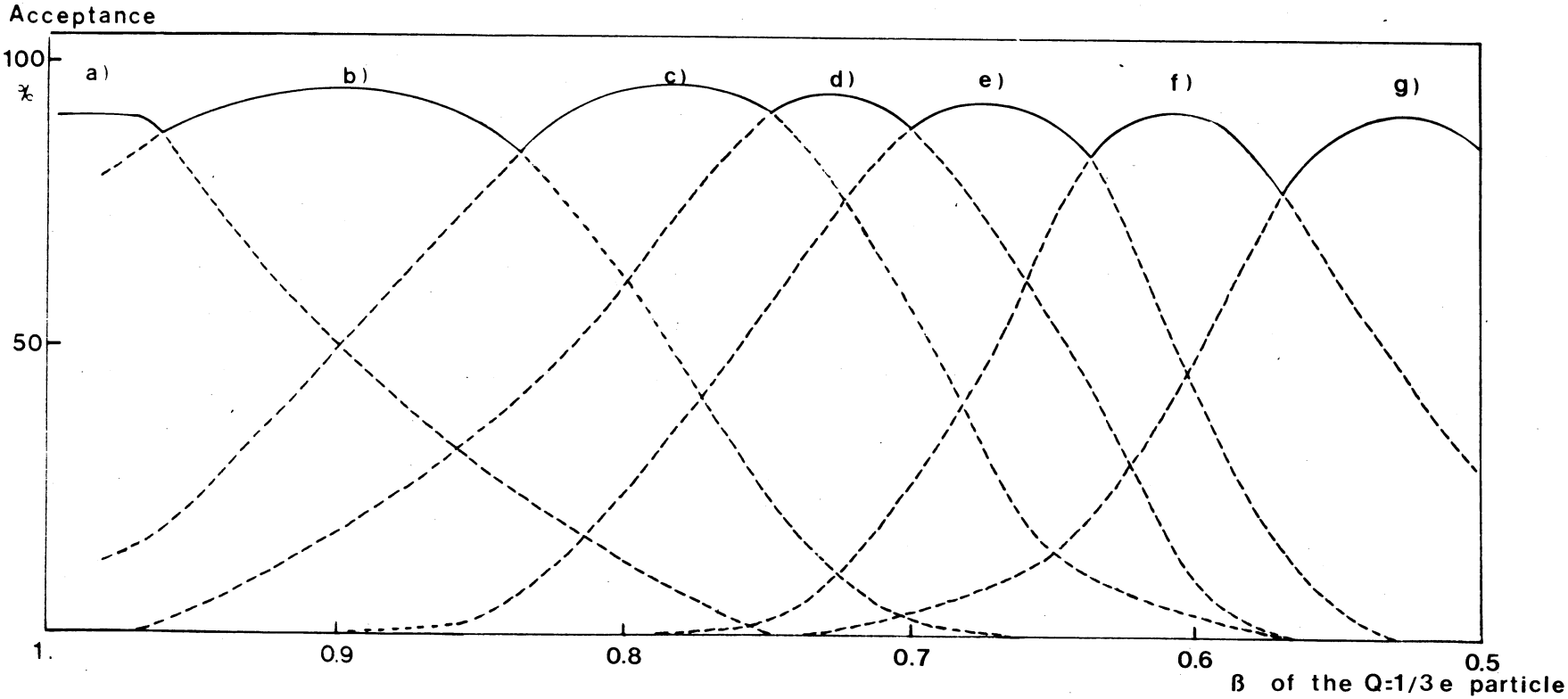
Acceptance
100
%
50
a)
b)
c)
d)
e)
f)
g)
1.
0.9
0.8
0.7
0.6
0.5
ß of the Q=1/3e particle

Fig. 2

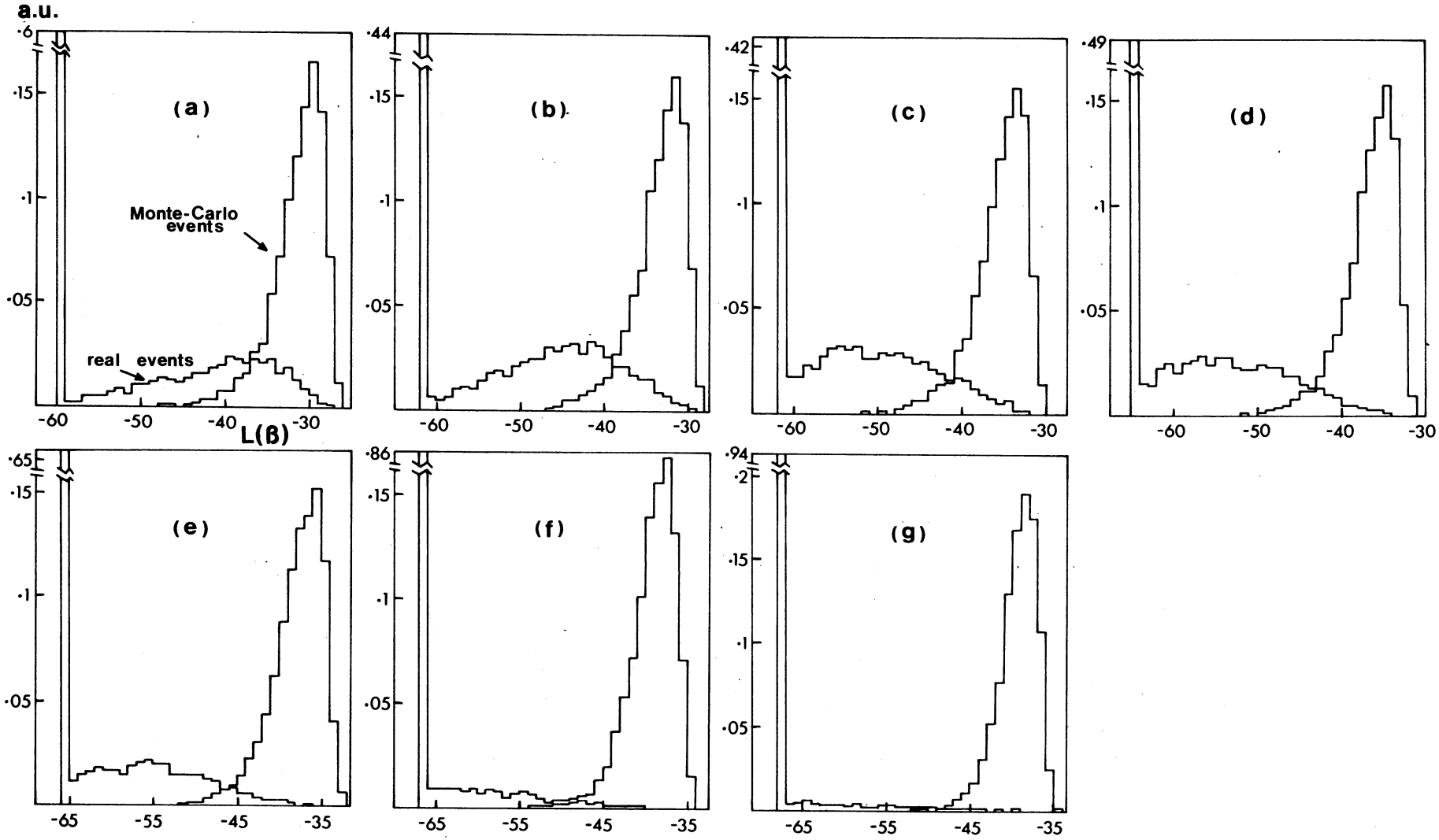

Fig. 3

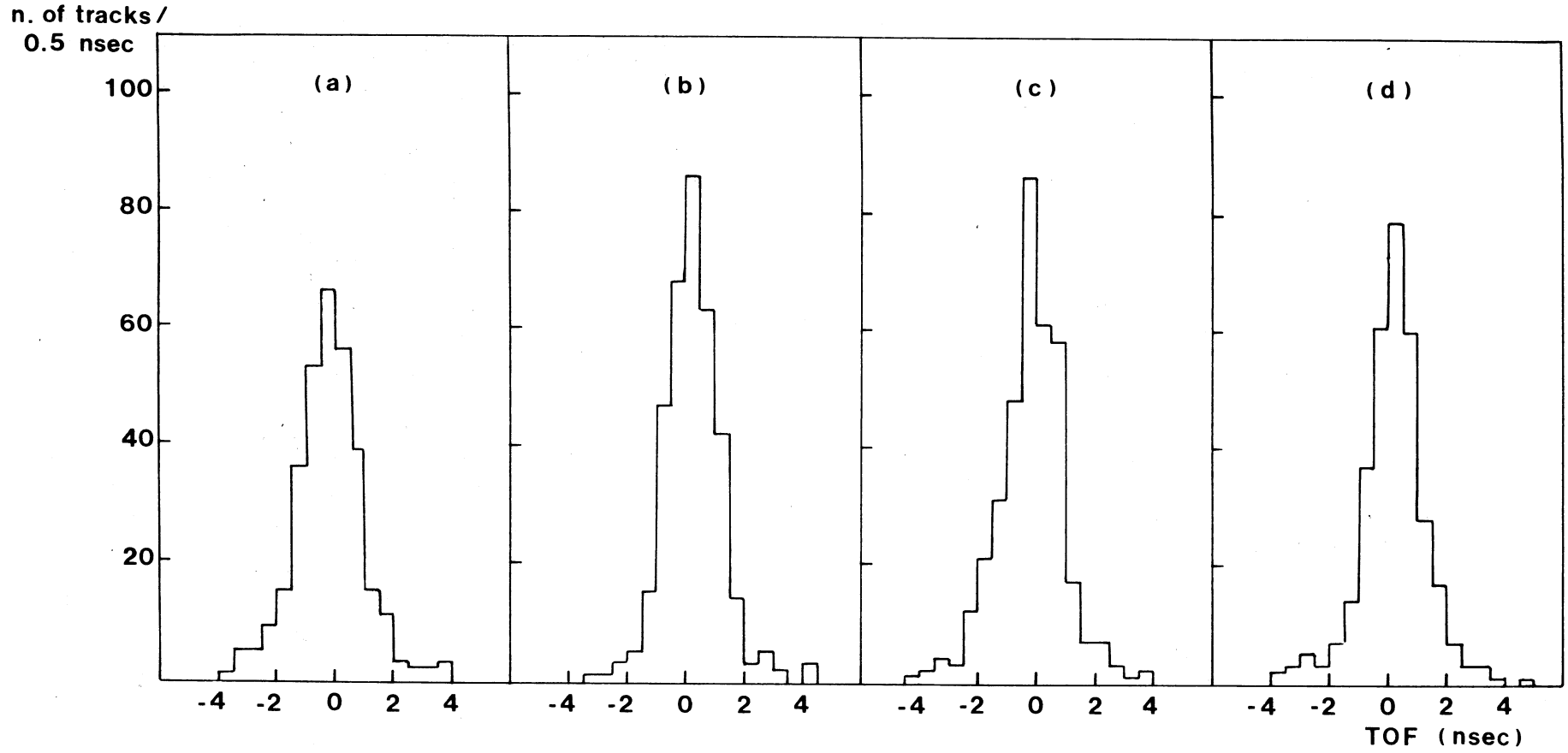

Fig. 4

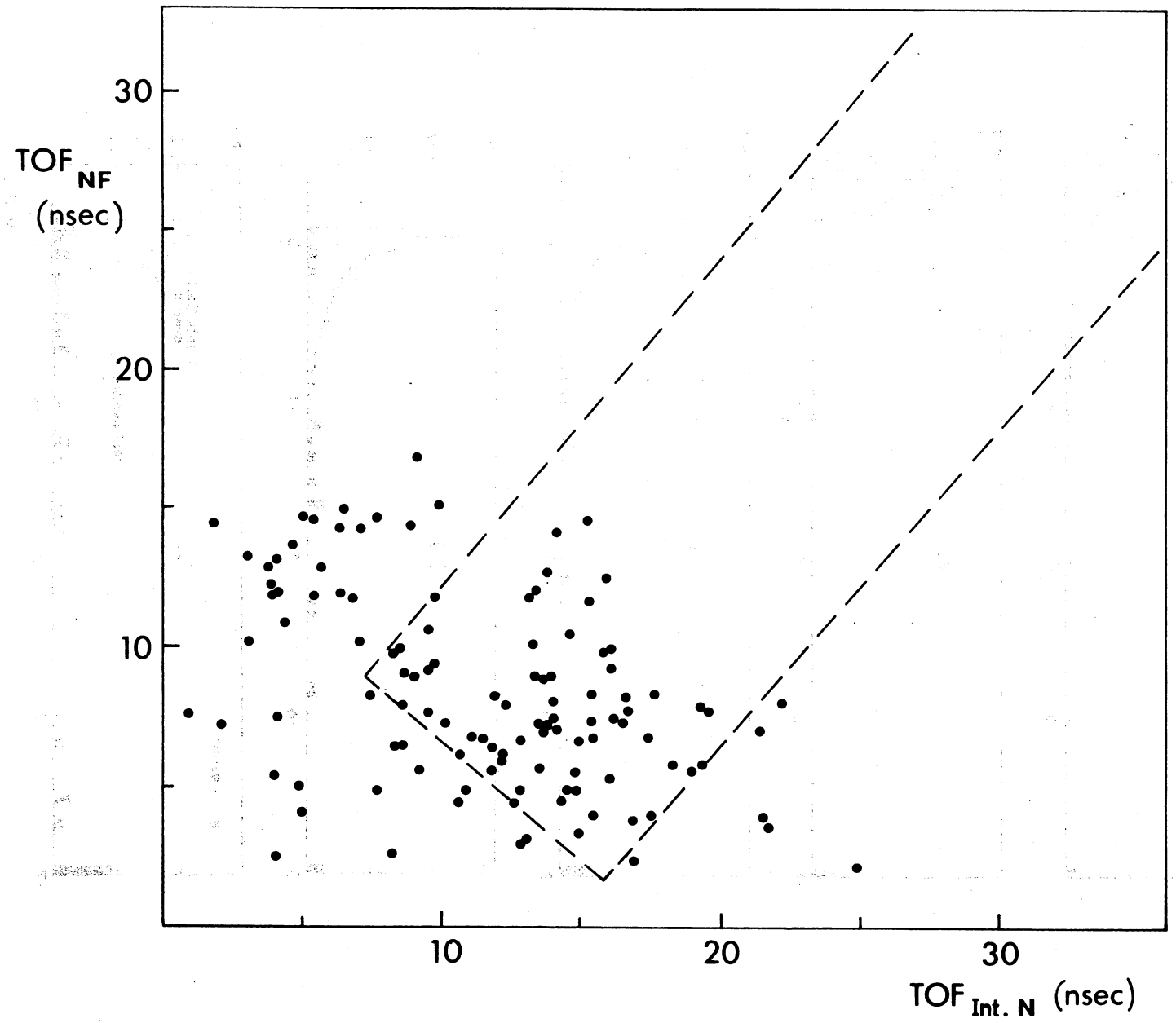

Fig. 5

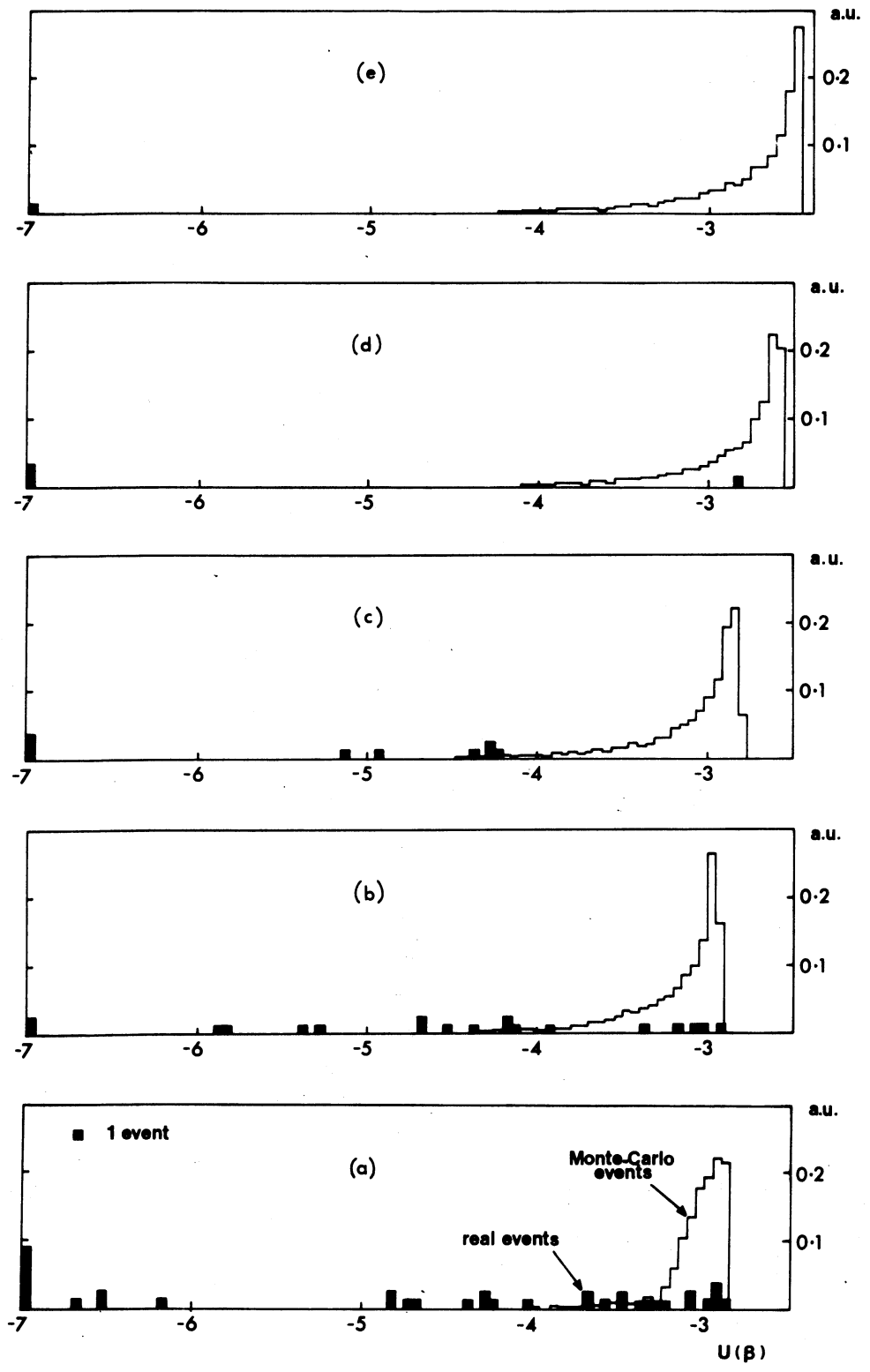
(e)
(d)
(c)
(b)
(a)
a.u.
0·2
0·1
-7
-6
-5
-4
-3
1 event
Monte-Carlo events
real events
U(β)

Fig. 6

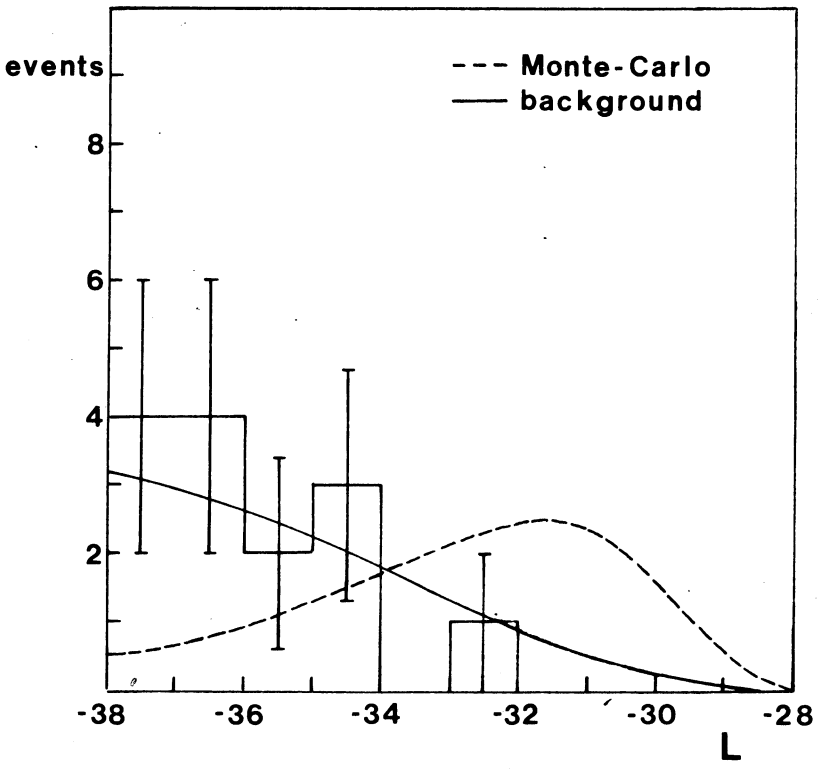

Fig. 7

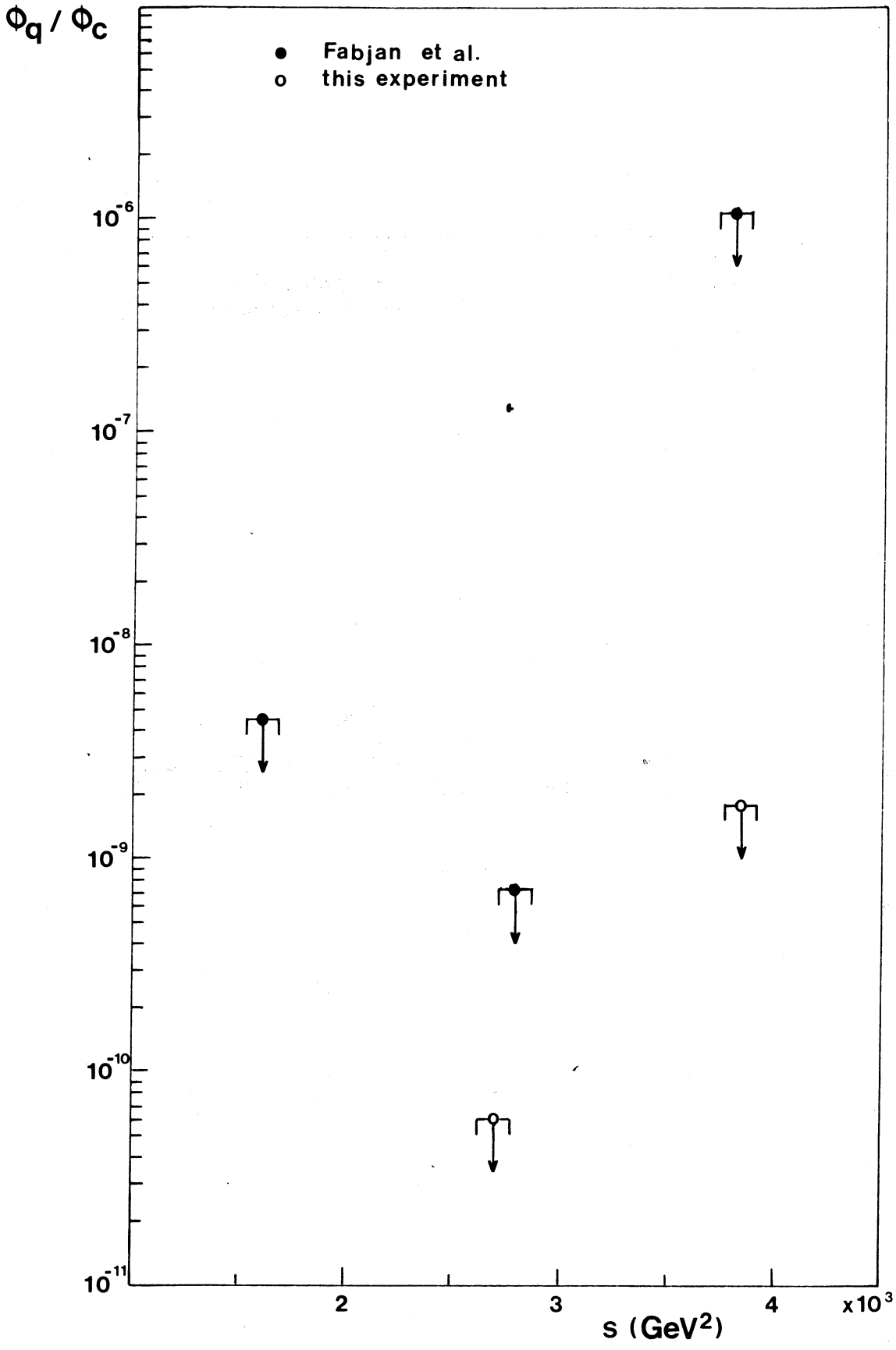
Φ_q / Φ_c
● Fabjan et al.
o this experiment
10^{-6}
10^{-7}
10^{-8}
10^{-9}
10^{-10}
10^{-11}
2
3
4
x10^3
s (GeV^2)

Fig. 8

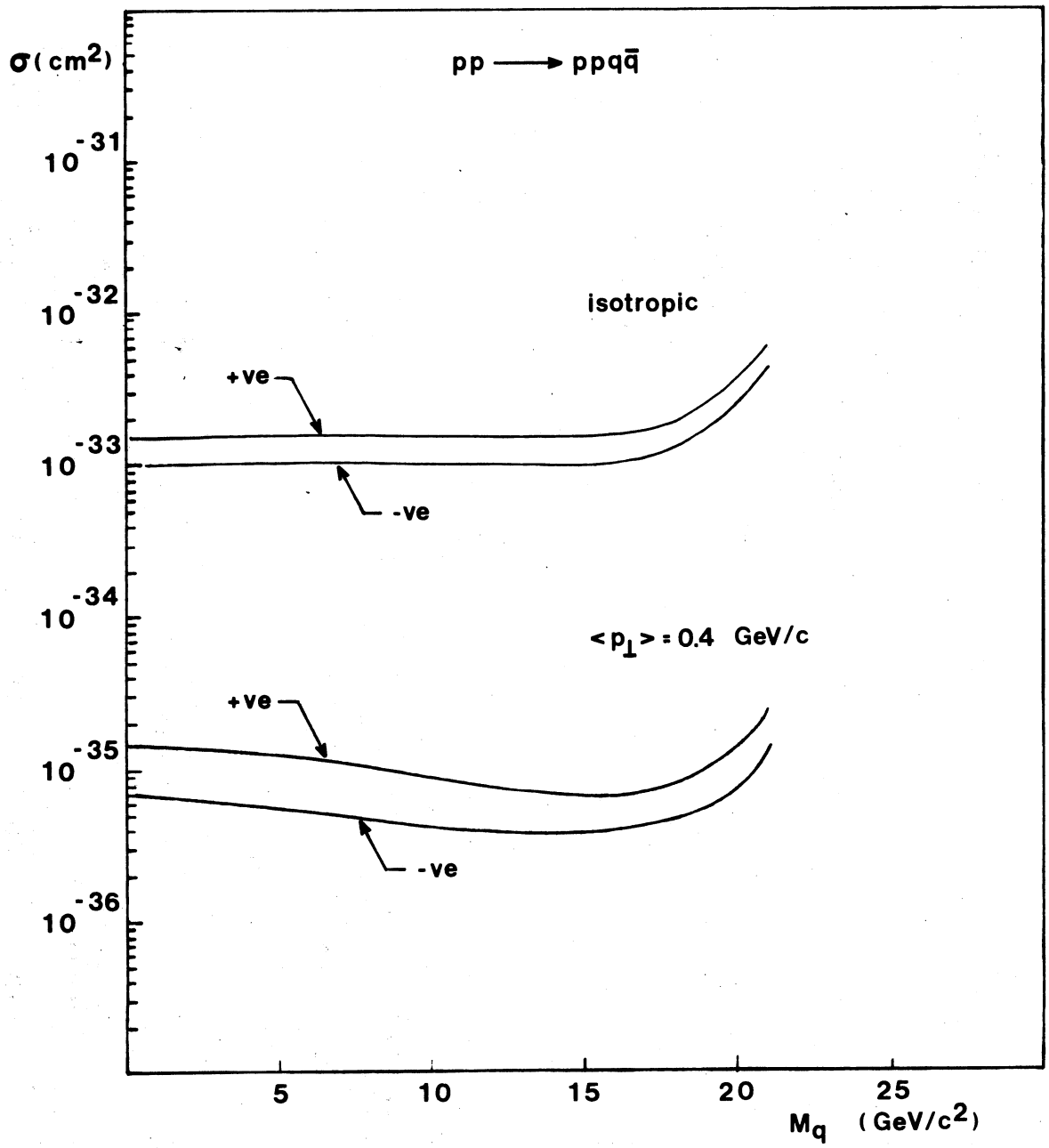
σ(cm²)
pp ⟶ ppqq̄
10⁻³¹
10⁻³²
isotropic
+ve
10⁻³³
-ve
10⁻³⁴
<p⊥> = 0.4 GeV/c
+ve
10⁻³⁵
-ve
10⁻³⁶
5
10
15
20
25
Mq (GeV/c²)

Fig. 9

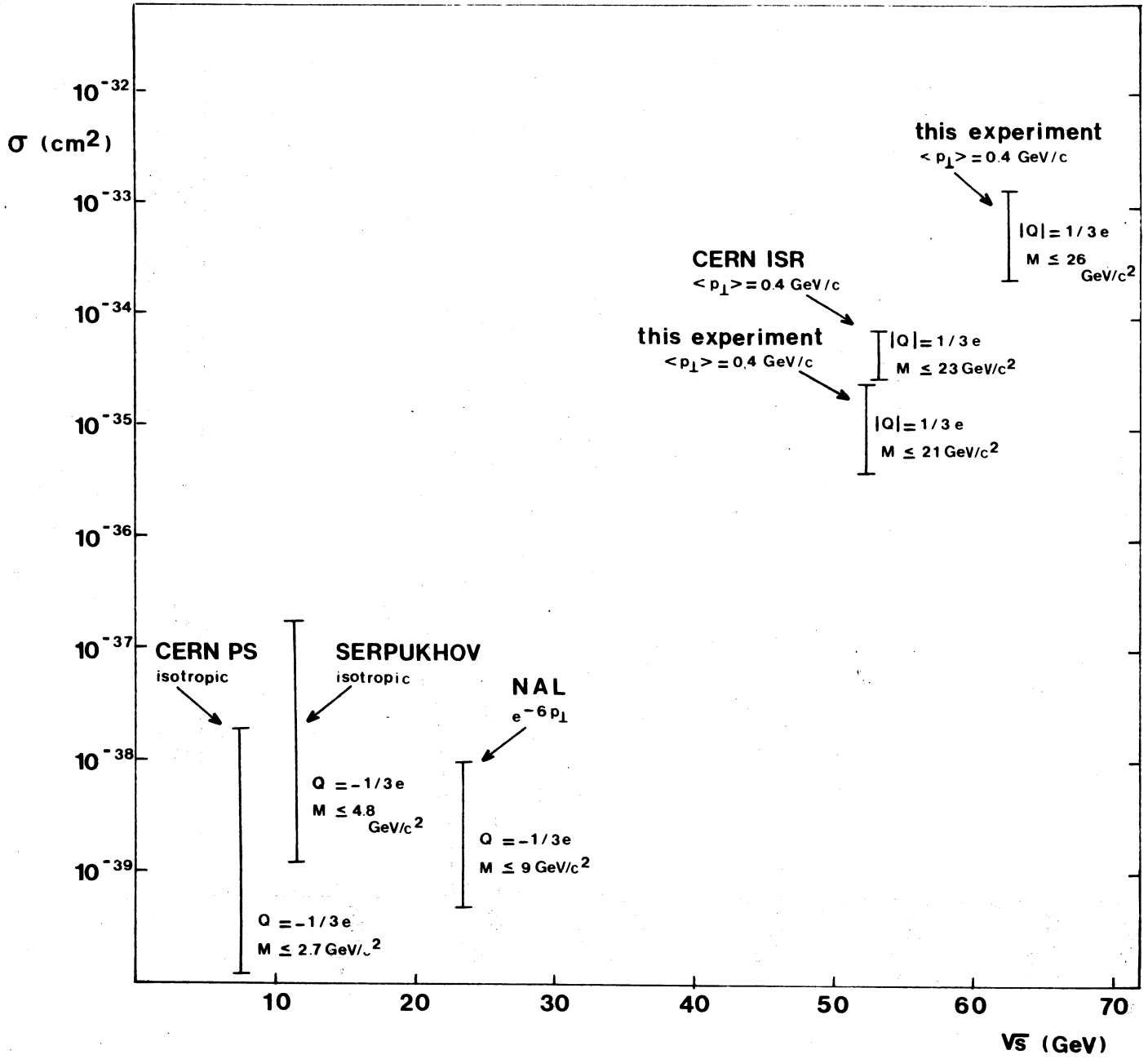
σ (cm²)
10⁻³²
10⁻³³
10⁻³⁴
10⁻³⁵
10⁻³⁶
10⁻³⁷
10⁻³⁸
10⁻³⁹
this experiment
< p⊥ > = 0.4 GeV/c
|Q| = 1/3 e
M ≤ 26 GeV/c²
CERN ISR
< p⊥ > = 0.4 GeV/c
this experiment
< p⊥ > = 0.4 GeV/c
|Q| = 1/3 e
M ≤ 23 GeV/c²
|Q| = 1/3 e
M ≤ 21 GeV/c²
CERN PS
isotropic
SERPUKHOV
isotropic
NAL
e⁻⁶ p⊥
Q = -1/3 e
M ≤ 4.8 GeV/c²
Q = -1/3 e
M ≤ 9 GeV/c²
Q = -1/3 e
M ≤ 2.7 GeV/c²
10
20
30
40
50
60
70
√s (GeV)

Fig. 10